Proc. Vth International Workshop, Advances in Signal Processing for Non Destructive Evaluation of Materials
Québec City (Canada),2-4 Aug. 2005. © X. Maldague ed., É. du CAO (2006), ISBN 2-9809199-0-X

Regularization approach for inverse problems in order to characterize defects by eddy current NDE

Stéphanie Dubost[1], Yves Goussard[2],Laurence Châtellier[1], Raphaël Guichard[2]

[1]EDF R&D, 6 quai Watier, 78401 CHATOU CEDEX, FRANCE,[2]Biomedical Engineering Institue, Ecole Polytechnique de Montréal, PO Box 6079, Station "Centre Ville", Montréal, Québec, CANADA

Abstract Usual NDE techniques do not produce estimates of the depth of a surface breaking defect when this depth is below 5 mm. We propose a method based on the regularization of inverse problems that allows one to characterize surface breaking defects from eddy current sensors measurements. This method is based on two steps: the first step is the estimation of the characteristics of the inspected medium. The second step is the estimation of the characteristics of the defect. The depth estimates obtained on experimental data are very satisfying.

Keywords – Inverse problems, regularization, eddy current, PSF, reconstruction

1 Introduction

Key power plant components must meet regulatory requirements throughout their lives. Should a defect be detected on a component, plant operators must characterize (e.g. position and evaluate) the defect precisely, and then determine whether the component should be replaced or repaired. Thus, the ability to position and size defects in those major components is a key issue for the life management of plants, from both technical and economical standpoints.

There is nowadays no satisfying NDE technique leading to a correct estimation of the depth of a surface breaking defect when this depth is under 5 mm. The usual technique, which is based on ultrasonic measurements, may indeed be efficient when the defect depth is over 5 mm but does not enable the operator to determine whether the depth is less than 1 mm or between 3 and 5 mm, for example. Such a classification between defects with small depth may however be important to determine the best action to be undertaken in terms of replacement or repair.

In this paper we propose an approach based on eddy current measurement processing, by considering the problem as a so called *inverse problem*. Provided that a defect is present, the aim is to reconstruct a map of material relative conductivity which afterwards enables the operator to estimate several characteristics of the defect, among which its depth.

2 Problem Statement

We consider an austenitic steel object to be inspected with the help of eddy current (EC) sensors. It is assumed that a surface breaking defect is present, that it is isolated from other ones and that its shape is roughly that of a slot or a crack.

An EC sensor is moved on the surface of the component area containing the defect, along lines perpendicular to the direction of the defect length. If no defect is present, the electric field measured by the EC sensor is constant, whereas presence of a defect produces a variation of the electric field. Our goal is to use the set of EC measurements $\boldsymbol{y}$ to estimate the distribution of relative conductivity $\boldsymbol{x}$ in the area of interest. The relative conductivity is defined as the ratio $(\sigma_0-\sigma)/\sigma_0$, where σ_0 and σ respectively denote the austenitic steel and defect conductivities. The latter being generally equal to zero, the relative conductivity can be assumed to be either 0 (no defect) or 1 (presence of a defect).

3 Method

3.1 Modeling assumptions

We adopt the three-dimensional (3D), discretized framework schematically depicted in Figure 1. The probe collects measurements close to the surface $k = 0$ of the unknown medium. Our approach is based on a linearized form of the relationship between relative conductivity values $\boldsymbol{x}$ and measurements $\boldsymbol{y}$ whose expression is derived using minimal assumptions. More precisely, the linearity of the phenomena implies that the measurements $\boldsymbol{y}$ can be expressed as the sum of the contributions $\boldsymbol{y}_k$; $1 \le k \le K$ of each layer (constant value of index k) of the unknown medium. K denotes the total number of layers. In addition, the medium is assumed to be infinite in the i and j directions; consequently, the phenomena within each layer are shift-invariant and can therefore be expressed as a two-dimensional (2D) convolution product. Using a matrix notation, we can write:

$$\mathbf{y}_k = \mathbf{H}_k \mathbf{x}_k = \mathbf{X}_k \mathbf{h}_k \tag{1}$$

where the components of the 2D point spread function (PSF) which characterizes layer k and the relative conductivity components of layer k are concatenated in vectors $\boldsymbol{h}_k$ and $\boldsymbol{x}_k$, respectively. Matrices $\boldsymbol{H}_k$ and $\boldsymbol{X}_k$ are built from the elements of $\boldsymbol{h}_k$ and $\boldsymbol{x}_k$ in order to implement a 2D convolution product. From the above equations, we obtain:

$$\boldsymbol{y} = \sum_{k=1}^{K} \boldsymbol{y}_k = \boldsymbol{H}\boldsymbol{x} + \boldsymbol{n} = \boldsymbol{X}\boldsymbol{h} + \boldsymbol{n} \tag{2}$$

where matrices $\boldsymbol{H}$ and $\boldsymbol{X}$ and vectors $\boldsymbol{x}$ and $\boldsymbol{h}$ are built by appropriate concatenation of quantities $\boldsymbol{H}_k$ $\boldsymbol{X}_k$ $\boldsymbol{x}_k$ and $\boldsymbol{h}_k$; $1 \le k \le K$, respectively and where $\boldsymbol{n}$ denotes a noise vector that represents all phenomena not accounted for by the model.

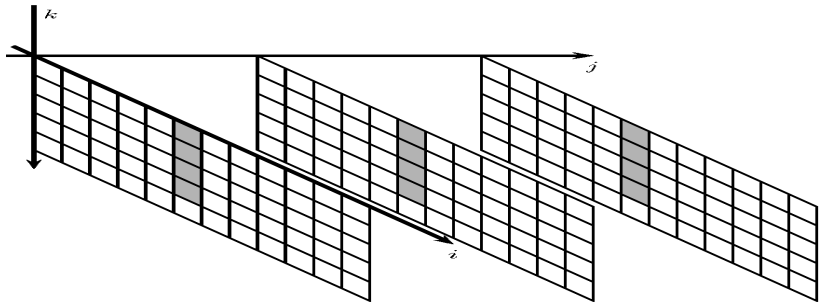

Figure 1 *Geometry of the discretized 3D problem. The probe collects measurements close to the surface k = 0 of the unknown medium.*

3.2 Approach

In the proposed approach, two stages are required: (*i*) utilization of actual data collected on known defects for estimating the set of PSFs which characterizes the probe/medium response; (*ii*) estimation of unknown defects using the PSFs obtained at the first stage. At both stages, the estimation problem is ill-conditioned in the sense that the information content and relative size of measured data is rather limited, with the consequence of a high sensitivity of the solutions to observation noise $\boldsymbol{n}$ [1]. In order to cope with this situation, some form of regularization must be used. Here regularization is achieved by using a *penalized least-squares estimator* at each stage. The penalty term is selected so as to produce an acceptable trade-off between some desirable properties of the estimates and the numerical efficiency of the resulting optimization procedure. These points are detailed in the next two sections.

3.3 PSF Estimation

Due to the nature of the underlying physical phenomena, we assume that each PSF of the set is smooth and that the shapes of the PSFs vary slowly with the depth index *k*. These characteristics can be encouraged by a quadratic penalty term on, e.g., the gradient of the estimate along the three axis directions. The corresponding penalized least-squares criterion takes the following form:

$$J(\boldsymbol{h};\boldsymbol{y}) = \|\boldsymbol{y} - \boldsymbol{X}\boldsymbol{h}\|^2 + \lambda\|\boldsymbol{D}\boldsymbol{h}\|^2 \tag{3}$$

where $\boldsymbol{D}$ represents the discrete gradient operator ($\boldsymbol{D}$ is actually the sum of the first difference operators along the three axis directions, with the possible addition of an operator proportional to identity) and where λ is a weighting parameter referred to as the *regularization parameter*. Note that the form $\boldsymbol{y} = \boldsymbol{X}\,\boldsymbol{h} + \boldsymbol{n}$ of the model is used at this stage as it is best suited to the estimation of vector $\boldsymbol{h}$. Note also that criterion $J(\boldsymbol{h};\boldsymbol{y})$ is quadratic with respect to $\boldsymbol{h}$ and that the solution can be expressed in closed form. However evaluation of the closed form solution is intractable in practice due to the size of matrices $\boldsymbol{X}$ and $\boldsymbol{D}$. In order to circumvent the difficulty, we chose to minimize $J(\boldsymbol{h};\boldsymbol{y})$ iteratively using a Polak-Ribiere conjugate gradient algorithm whose generic form is given in Table 1 [2]. At this stage, no preconditioning was applied ($\boldsymbol{M} = \boldsymbol{I}$). Derivation of the expression of the gradient of $J(\boldsymbol{h};\boldsymbol{y})$ is straightforward from the above equation and the optimal stepsize α (i.e., the stepsize value that produce the maximal decrease of the criterion at each iteration) can also be expressed rather easily in closed form. Finally, the value of regularization parameter λ can be determined either heuristically or using estimation techniques such as generalized cross-validation [3].

$$\begin{array}{rcl}
\boldsymbol{g}^{(n)} & = & -\nabla J(\boldsymbol{x}^{(n)}) \\
\boldsymbol{p}^{(n)} & = & \boldsymbol{M}\boldsymbol{g}^{(n)} \\
\gamma^{(n)} & = & \begin{cases} 0 & \text{si} \quad n = 0 \\ \dfrac{(\boldsymbol{g}^{(n)} - \boldsymbol{g}^{(n-1)})^{\mathrm{t}}\ \boldsymbol{p}^{(n)}}{(\boldsymbol{g}^{(n-1)})^{\mathrm{t}}\ \boldsymbol{p}^{(n-1)}} & \text{si} \quad n > 0 \end{cases} \\
\boldsymbol{d}^{(n)} & = & \boldsymbol{p}^{(n)} + \gamma^{(n)}\boldsymbol{d}^{(n-1)} \\
\boldsymbol{x}^{(n+1)} & = & \boldsymbol{x}^{(n)} + \alpha^{(n)}\boldsymbol{d}^{(n)}
\end{array}$$

Table 1 *Generic form of the Polak-Ribiere conjugate gradient algorithm used in this study. The quantity to be estimated is denoted by* $\boldsymbol{x}$*.* $\boldsymbol{M}$*, n and* α *represent the preconditioning matrix, the iteration index and the stepsize, respectively.*

3.4 Reconstruction of the unknown medium

The approach to the estimation of $\boldsymbol{x}$ when the PSFs are known is essentially similar to the one described in the previous paragraph. However, the defects car hardly be considered smooth since they are made up of homogeneous regions separated by sharp discontinuities. In order to account for this characteristic, the penalty term is based upon an *edge-preserving, convex potential function* φ applied to all components and differences between pairs of neighboring components of $\boldsymbol{x}$. Function $\varphi(u) = (s^2+u^2)^{1/2}$, where *s* represents a scale factor, is essentially similar to the Huber function used in edge-preserving image reconstruction [4]. Therefore, the penalized least-squares criterion used for reconstructing unknown defects takes the following form:

$$J(\boldsymbol{x};\boldsymbol{y}) = \|\boldsymbol{y} - \boldsymbol{H}\boldsymbol{x}\|^2 + \lambda_0\varphi(\boldsymbol{x}) + \lambda_1\varphi(\boldsymbol{D}\boldsymbol{x}) \tag{4}$$

where, for any vector $\boldsymbol{v}$, the notation $\varphi(\boldsymbol{v})$ is used in place of $\Sigma\varphi(v_i)$, the summation being extended to all components of $\boldsymbol{v}$. λ_0 and λ_1 denote the regularization parameters and $\boldsymbol{D}$ represents the same

gradient operator as in the previous paragraph. Note that at this stage, the form $\boldsymbol{y} = \boldsymbol{H}\,\boldsymbol{x} + \boldsymbol{n}$ of the model is used because it is best suited to the estimation of $\boldsymbol{x}$.

As indicated above, the non-quadratic penalty term in (4) better expresses a salient characteristic of the defects to be reconstructed. Criterion $J(\boldsymbol{x};\boldsymbol{y})$ remains convex and coercive, which guarantees the existence of a unique minimum and is a necessary condition for convergence of iterative descent algorithms toward this unique minimum. However, in general, this convergence is slower than in the quadratic case; in addition, the solution can no longer be expressed in closed form and neither can the stepsize of conjugate gradient techniques.

In order to minimize $J(\boldsymbol{x};\boldsymbol{y})$, we selected the same conjugate gradient algorithm as at the first stage because of its adequate trade-off between numerical efficiency, convergence speed and ease of implementation. In order to speed up the convergence, preconditioning was applied in the form of the inverse of the Hessian of the quadratic term of criterion (4). The gradient can be computed easily, thanks to the simple analytical expression of φ. The stepsize α at each iteration was determined using a simple and fast iterative search [2]. Finally, the regularization parameters where determined in a heuristic manner from the reconstruction of known test defects.

4 Results

4.1 Experimental data

The probe used in our experiments was an air cored coil with a 3.5 mm external diameter used in impedance mode at frequency 300kHz. The acquisition step was equal to 0.2 mm. The experimental data were obtained by inspection of austenitic stainless steel 304L slabs, on which several notches had been electro-eroded. The notches characteristics were: length (15 or 20 mm), width (0.1, 0.2 or 0.3 mm), depth (0.5, 1, 2, 3, 4, 5, 6 mm), and shape (rectangular or semi-elliptical). The discretization step of the medium was equal to 0.2 mm along directions *i* and *j*, and to 0.5 mm along direction *k*. The relative conductivity was estimated up to an 8 mm depth, which corresponds to 16 layers along direction *k*.

4.2 PSF estimation

4.2.1 Main settings

In a preliminary step, one must *select a data set* from which the PSFs will be estimated. At the PSF estimation stage, the rectangular notches with length 15mm and width 0.2mm were used. As the choice of a data set is not obvious, two data sets leading to two PSF estimates were compared. The first data set contained notches with depths 1, 3, 6 mm, the second one contained notches with depths 0.5, 1, 2, 3, 4, 5, 6 mm. The quality of reconstruction results obtained with the two PSFs was quite identical (slightly better for the first set). This seems to indicate that the data set used must be chosen so that each data provides additional information, which is probably not the case for the second set. The results presented in this paper are obtained with the PSF estimated on the first set.

The *PSF size* must also to be set before performing the estimation. As there was no isolated point defect in the data set, the PSF size could not be assessed by direct observation of the measurements. Selection of the PSF size was performed by making sure that the PSF decreased correctly toward zero at their support boundaries. Another way is to synthesize data from the estimated PSFs corresponding to different sizes, and compare them with the real data. Here, the selected sizes here were 13.4 x 8.2 mm along the the *i* and *j* directions.

In our experiments, the value of *regularization parameter* λ that appears in (3) was set heuristically by observing the shape of the estimated PSFs: not enough regularization seems to produce “noisy”

estimates whereas too much regularization leads to too “flat” PSFs. Once this physically PSF aspect is accounted for, one can refine parameter values by comparing synthesized data with real ones.

4.2.2 PSF estimation results

An example of PSF estimation result is given in Figure 2. Two PSF layers are shown: left, the PSF corresponding to the first layer (depth between 0 and 0.5 mm), and right the PSF corresponding to the sixth layer (depth between 2.5 and 3 mm).

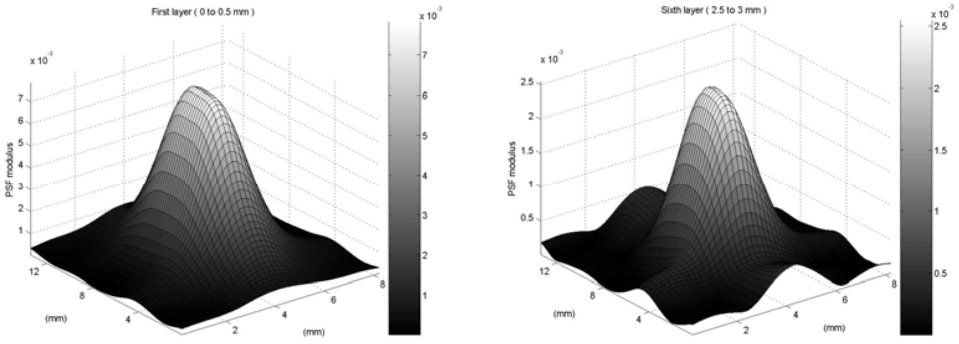

Figure 2 *Modulus of the first (left hand side) and sixth (right hand side) layer of the estimated PSF*

The estimated PSF have roughly the same shape. Both the magnitude and the support region are larger for layers closer to the surface. We observed that, for deeper layers, the PSF estimates seem to be less regular near the edges.

4.3 Reconstruction of the unknown medium

4.3.1 Main settings

At this stage also, the regularization parameters that appear in (4) must be set before performing the reconstruction. Here too, we used a heuristic approach in which some known defects (in our case: two) were reconstructed for different hyperparameter values. By dichotomy, we choose the parameters that gave the best results in terms of contrast (the reconstruction is as clean as possible) and precision (the estimated characteristics are as close to the real ones as possible). Then, those regularization parameters values were fixed and used for all other reconstructions.

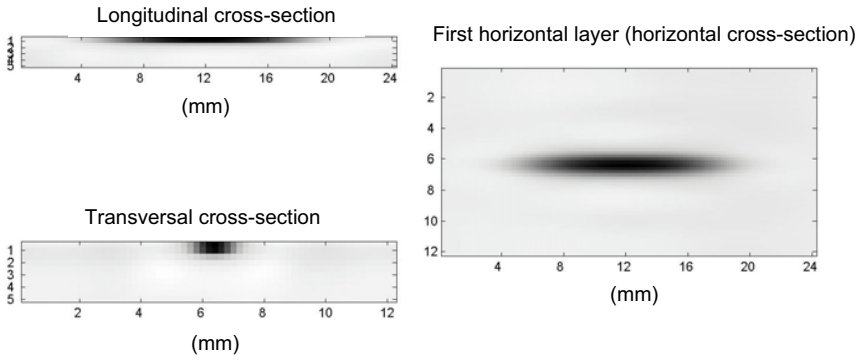

Figure 3 *Longitudinal, transversal and horizontal cross-sections of the estimated relative conductivity for the medium containing a rectangular slot with depth 1 mm, length 15 mm, width 0.2 mm*

4.3.2 Reconstruction results

The reconstruction results were obtained from data different from the ones used at the PSF estimation stage. An example of reconstruction result is shown in Figure 3. The defect was a rectangular slot with length 15 mm, depth 1 mm, width 0.2 mm (These characteristics are identical to those of a defect used at the PSF estimation stage, but the data were provided by another inspection of the same slab). Three cross-sections are presented (longitudinal, transversal, horizontal) in order to assess the geometry of the defect properly. It can be observed that the reconstruction leads to overestimation of the width, but to satisfactory depth and length estimation.

Additional reconstruction results obtained with 10 other defects are summarized in Table 2. The actual and estimated dimensions of the defects are reported, except for the estimated width which was systematically overestimated (in the order of 0.6 mm).

Shape	rectangular	rectangular	rectangular	rectangular	semi-elliptic	semi-elliptic	rectangular	rectangular	rectangular	rectangular
Depth	1	3	1	3	1	3	1	0.5	3	4
Length	15	15	20	20	15	15	15	15	15	15
Width	0.2	0.2	0.2	0.2	0.2	0.2	0.1	0.2	0.3	0.2
Estimated Depth	~ 1	~ 2.5	~ 1	~ 3	~ 1	~ 2	~ 1.5	~ 1	~ 1.5	~ 3.5
Estimated length	~ 15	~ 15	~ 20	~ 20	~ 10	~ 12	~ 14	~ 14	~ 14	~ 15

Table 2 *Reconstruction results for different slots*

The following conclusions can be drawn from these and other experiments performed in similar conditions: the *depth* and *length* are correctly estimated for rectangular slots, and slightly underestimated for semi-elliptic slots; the width is systematically overestimated; the shape of the reconstructed defect is not really relevant of the real shape, as it is roughly the same for all defects.

5 Conclusion and perspectives

In this paper we presented a method based on the regularization of inverse problems that provides estimates of the characteristics of unknown defects. The results are satisfying as the main goal, which was to estimate depths defect below 5 mm, seems to be reached at least for rectangular slots.

Some further inverstigations are in progress in order to improve both methodological and practical aspects. We are indeed working on the improvement of the reconstruction step based on other regularization functions. Practical application of this method to real defects coming from plant components is also in progress.

6 References

[1] G. Demoment, “Image Reconstruction and Restoration: Overview of Common Estimation Structure and Problems,” *IEEE Trans. Acoustics, Speech and Signal Proc*., vol. ASSP-37, no 12, pp. 2024-2036, 1989.

[2] J. A. Fessler and S. D. Booth, “Conjugate-Gradient Preconditioning Methods for Shift-Variant PET Image Reconstruction,” *IEEE Trans. Image Proc.*, vol. 8, no 5, pp. 688-699, 1999.

[3] G. H. Golub, M. Heath and G. Wahba. “Generalized Cross-Validation as a Method for Choosing a Good Ridge Parameter,” *Technometrics*, vol. 21, no. 2, pp. 215-223, 1979.

[4] A. H. Delaney and Y. Bresler, “Globally Convergent Edge-Preserving Regularized Reconstruction: An Application to Limited-Angle Tomography,” *IEEE Trans. Image Proc.*, vol. 7, no 2, pp. 204-221, 1998.